# 2
# A simple example

In this chapter we are going to discuss a simple case in which a quantum field theory simulates the effect of Pomeron exchange in the Regge limit of

$$s \gg |t|.$$

We do not mean that we can identify a Regge trajectory, with associated bound states for various values of positive $t$, but rather that in this limit the scattering amplitude has the form

$$A(s,t) \propto s^{\alpha_P(t)}. \tag{2.1}$$

The model we shall consider here is not QCD, but a much simpler quantum field theory, namely a scalar field theory with cubic interactions. We shall show that by summing perturbative contributions to all orders in the coupling constant, but *keeping only leading logarithms*, the behaviour expressed by Eq.(2.1) does indeed emerge. By 'leading logarithms' , we refer to those terms in the perturbative expansion which contain important (in the high energy limit) $\ln s$ factors. Precisely which terms we keep will become clear as we develop the calculation.

An example of Pomeron behaviour from a scalar theory with cubic interactions has been considered before, for example by Polkinghorne (1963a–c) which is described in *The Analytic S-Matrix* by Eden, Landshoff, Olive & Polkinghorne (1966). Their treatment is something more straightforward than the method we shall be introducing here. Feynman diagrams are calculated using the usual method of Feynman parametrization and ladder diagrams are readily summed to all orders. The alternative method that we shall be using here is closer to the treatment by Chang & Yan (1970, 1971). It is something of a sledgehammer to crack a nut. However, the techniques that we shall introduce will serve well in



https://doi.org/10.1017/9781009290111.004 Published online by Cambridge University Press

future chapters when they are applied to the more realistic case of QCD.

## 2.1 The model

We shall represent quarks (and antiquarks) by a complex scalar field $\phi$ and gluons by another scalar field $\chi$. In order to avoid the difficulty of infra-red divergences (which will be discussed at length in future chapters) we shall assign a mass $m$ to the gluons (whilst leaving the quarks massless). The gluons can interact with themselves as well as with the quarks. A cubic interaction between scalar fields has dimension of mass. In order to introduce a dimensionless coupling constant $g$, we shall factor out a mass $m$ from the cubic couplings.

A minor complication occurs when considering the analogue of the colour $SU(N)$ group, which is the gauge group of QCD ($N=3$, but in what follows we keep the number of colours general so as to expose the colour factors explicitly). The self-interaction term in the Lagrangian of the scalar gluons must be symmetric under interchange of two (bosonic) gluons, but we would like the interaction vertex to be proportional to the structure constants of the colour group (which are antisymmetric under interchange of colour indices). This leads us to introduce a colour group which is a product of two $SU(N)$ groups. Thus the gluon fields carry two colour indices and are denoted by $\chi^{a,r}$ with $a, r = 1 \cdots (N^2-1)$. The quark field transforms in the fundamental representation of both of these $SU(N)$ groups and so also carries two indices, i.e. $\phi_{i,l}$ with $i, l = 1 \cdots N$. This is rather cumbersome, but in fact the colour factors are in general quite easy to keep track of (and at least there will be some feature which is simpler in QCD!).

Thus the Lagrangian density for this model may be written

$$\begin{aligned} \mathcal{L} &= \partial^\mu \bar{\phi}^{i,l} \partial_\mu \phi_{i,l} + \frac{1}{2} \partial^\mu \chi_{a,r} \partial_\mu \chi^{a,r} - \frac{m^2}{2} \chi_{a,r} \chi^{a,r} \\ &\quad - gm \bar{\phi}^{i,l} (T^a)_i^j (T^r)_l^m \phi_{j,m} \chi_{a,r} - \frac{gm}{3!} f_{abc} f_{rst} \chi^{a,r} \chi^{b,s} \chi^{c,t}, \end{aligned}$$

where the matrices $T^a$ and $T^r$ are the generators of the two $SU(N)$ groups whose structure constants are $f_{abc}$ and $f_{rst}$ respectively.

https://doi.org/10.1017/9781009290111.004 Published online by Cambridge University Press

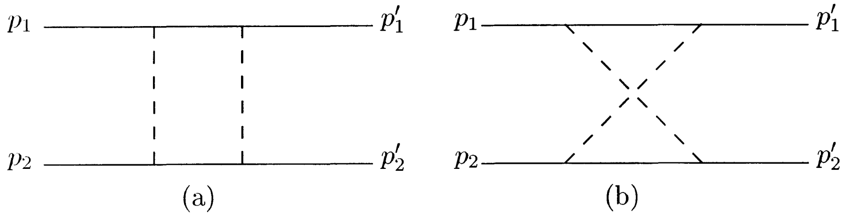


Fig. 2.1. Leading order contribution to Pomeron exchange.

Thus

$$\left[T^a, T^b\right] = i f_{abc} T^c, \quad [T^r, T^s] = \; i f_{rst} T^t. \tag{2.2}$$

We do not have an analogue of the quartic coupling between gluons. It turns out that in QCD these interactions always give contributions which are sub-leading in $\ln s$ and we therefore neglect them. We can also assume that the quark fields carry a flavour index which we have suppressed.

Within the context of this model we shall now calculate to all orders in perturbation theory, but keeping the leading powers of $\ln s$ in each order, the process of quark–quark scattering via the exchange of a colour singlet. We assume that the two quarks have different flavours and they emerge from the scattering with the same colour with which they entered.

## 2.2 The leading order contribution

The leading order Feynman diagrams contributing to this process are shown in Fig. 2.1. The quark lines are denoted by solid lines and the gluons by dashed lines. Because the quarks have different flavours we do not have to consider diagrams with quarks exchanged in the $t$-channel.

The ingoing quarks have momenta $p_1$ and $p_2$, respectively, and the outgoing quarks have momenta $p_1'$ and $p_2'$ respectively. Since we are interested in purely elastic scattering we need to consider graphs which do not alter the colour of the incoming quarks, i.e. colour singlet exchange. Therefore there is no contribution to the process in which only one gluon is exchanged and the minimum number of exchanged gluons must be two. The second diagram

https://doi.org/10.1017/9781009290111.004 Published online by Cambridge University Press

(Fig. 2.1(b)) is related to the first by interchange of the incoming and outgoing lower quark lines. The colour generators on the lower line are reversed, but since we are concerned with colour singlet exchange, the two diagrams have the same colour factor. Thus the only difference comes from the kinematics. In other words by crossing symmetry it is sufficient to calculate the contribution from Fig. 2.1(a) and obtain the other contribution from the interchange of the Mandelstam variables $s$ and $u$ (which is equivalent to the interchange of $p_2$ and $p_2'$).

We deal first with the colour factor. This is straightforward. For a colour singlet exchange we obtain a factor for *each* of the $SU(N)$ groups of

$$\frac{1}{N^2}\mathrm{Tr}(T^aT^b)\mathrm{Tr}(T^aT^b) \;=\; \frac{N^2-1}{4N^2},$$

giving an overall colour factor of

$$\frac{(N^2-1)^2}{16N^4}. \qquad (2.3)$$

Fig. 2.1(a) is a one loop diagram, which can be calculated by the conventional means of Feynman parametrization, and the leading logarithm term $\ln(s/t)$ can be extracted from the integral over Feynman parameters. However, it turns out in general to be much more convenient to use dispersive techniques, i.e. we apply the Cutkosky rules (Cutkosky (1960)), which tell us that the imaginary part of this amplitude can be related to a phase-space integral of a product of two amplitudes at the tree level (see Eq.(1.1) and Fig. 1.1), i.e.

$$\Im\mathrm{m}\mathcal{A}_{(2.1a)} \;=\; \frac{1}{2}\int d\left(P.S.^2\right)\mathcal{A}_0^{(g)}(k)\mathcal{A}_0^{(g)\dagger}(k-q), \qquad (2.4)$$

where $\mathcal{A}_0^{(g)}$ is the tree amplitude for single gluon exchange shown either side of the cut in Fig. 2.2, i.e.

$$\mathcal{A}_0^{(g)}(k) \;=\; -g^2m^2\frac{1}{(k^2-m^2)}$$

up to a colour factor. $\mathcal{A}_0^{(g)\dagger}$ is the hermitian conjugate of the amplitude, i.e. the complex conjugate of the amplitude with the signs of the momenta reversed. The vector $q^\mu$ is the momentum transferred and so $t = q^2$. The symbol $d\left(P.S.^2\right)$ means the integral over

https://doi.org/10.1017/9781009290111.004 Published online by Cambridge University Press

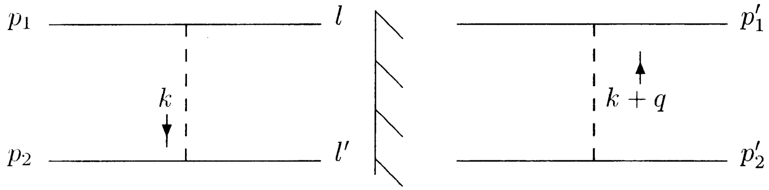


Fig. 2.2. Imaginary part of Fig. 2.1(a). We adopt the convention that $t$-channel momenta on the left of the cut are directed *downwards*, whereas $t$-channel momenta on the right of the cut are directed *upwards*.

the phase space of the two cut lines (whose momenta are $l$ and $l'$), i.e.

$$\int d\left(P.S.^2\right) = \int \frac{d^4l}{(2\pi)^3}\frac{d^4l'}{(2\pi)^3}\delta(l^2)\delta(l'^2)(2\pi)^4\delta^4(p_1+p_2-l-l').$$

One of these integrals (say $d^4l'$) can be used to absorb the energy-momentum conserving delta function $\delta^4(p_1+p_2-l-l')$ and, for the other, it is convenient to integrate not over the momentum of the other outgoing particle, but over the momentum $k$ of the exchanged gluon. Thus we have

$$\int d\left(P.S.^2\right) = \frac{1}{(2\pi)^2}\int d^4k\ \delta((p_1-k)^2)\ \delta((p_2+k)^2).$$

Now we parametrize the momentum $k$ in terms of **Sudakov parameters** $\rho$ and $\lambda$:

$$k^\mu = \rho p_1^\mu + \lambda p_2^\mu + k_\perp^\mu,$$

where $k_\perp^\mu$ is the momentum transverse to $p_1$ and $p_2$ and we represent this two-dimensional vector by the boldface $\mathbf{k}$. In other words in the centre-of-mass frame in which the incoming particles are considered to be along the $z$-axis we have

$$p_1^\mu = \left(\frac{\sqrt{s}}{2},\frac{\sqrt{s}}{2},\mathbf{0}\right),$$

$$p_2^\mu = \left(\frac{\sqrt{s}}{2},-\frac{\sqrt{s}}{2},\mathbf{0}\right),$$

$$k^\mu = \left((\rho+\lambda)\frac{\sqrt{s}}{2},(\rho-\lambda)\frac{\sqrt{s}}{2},\mathbf{k}\right).$$

https://doi.org/10.1017/9781009290111.004 Published online by Cambridge University Press

Using $s = 2p_1 \cdot p_2$ and performing the change of variables the phase-space integral becomes

$$\int d\left(P.S.^2\right) = \frac{s}{8\pi^2}\int d\rho\, d\lambda\, d^2\mathbf{k}\, \delta(-s(1-\rho)\lambda-\mathbf{k}^2)\, \delta(s(1+\lambda)\rho-\mathbf{k}^2). \tag{2.5}$$

In the limit $|t| \ll s$ the momentum transferred $q^\mu$ is dominated by its transverse component (i.e. $t = q^2 \approx -\mathbf{q}^2$), as can easily be checked from the requirement that the outgoing particles on the right hand side of Fig. 2.2 must be on their mass-shell. Similarly the magnitude of $\mathbf{k}$ will also be of the order of the larger of $m$ and $\sqrt{|t|}$ (it is unlikely that the momentum transferred in the two parts of the diagram on either side of the cut will be much larger than $\sqrt{|t|}$ in such a way that the sum of the two transverse momentum vectors gives $\mathbf{q}$). Thus the delta functions in Eq.(2.5) which give $\lambda = -\rho$ and $\rho \approx \mathbf{k}^2/s$ tell us that both $\rho$ and $|\lambda|$ are both of order $-t/s$ and very much smaller than 1. This means that $k^2$ may be approximated by

$$k^2 \approx -\mathbf{k}^2$$

and similarly

$$(k-q)^2 \approx -(\mathbf{k}-\mathbf{q})^2.$$

Absorbing the delta functions to perform the integration over $\rho$ and $\lambda$:

$$\Im\mathrm{m}\mathcal{A}_{(2.1a)} = \frac{(N^2-1)^2}{16N^4}\frac{g^4m^4}{16\pi^2 s}\int d^2\mathbf{k}\frac{1}{(\mathbf{k}^2+m^2)}\,\frac{1}{\left((\mathbf{k}-\mathbf{q})^2+m^2\right)}. \tag{2.6}$$

The integral over the transverse momentum, $\mathbf{k}$, is readily performed. We choose not to do it here, rather we want to write Eq.(2.6) as

$$\Im\mathrm{m}\mathcal{A}_{(2.1a)} = \frac{(N^2-1)^2}{16N^4}\frac{g^4m^4}{16\pi^2 s}\int d^2\mathbf{k}\, f_0(\mathbf{k},\mathbf{q}), \tag{2.7}$$

where

$$f_0(\mathbf{k},\mathbf{q}) = \frac{1}{(\mathbf{k}^2+m^2)}\,\frac{1}{\left((\mathbf{k}-\mathbf{q})^2+m^2\right)}. \tag{2.8}$$

The reason for this apparently perverse notation will become clear when we go on to consider higher order contributions.

https://doi.org/10.1017/9781009290111.004 Published online by Cambridge University Press

The imaginary part then immediately gives us the coefficient of the term $\ln(s/t)$, simply by using the relation (noting that $s/t$ is *negative*):

$$\ln\left(\frac{s}{t}\right) = \ln\left(\frac{s}{|t|}\right) - i\pi.$$

In Eq.(2.6) we have computed the coefficient of the $i\pi$ and the mere existence of an imaginary part tells us that there must be a logarithm in the real part with equal and opposite coefficient. However, we note that when the contribution from Fig. 2.1(b) is added, the large logarithm cancels and we are left with only the imaginary part. This is seen by observing that the contribution to Fig. 2.1(a) is proportional to

$$\frac{1}{s}\left(\ln\left(\frac{s}{|t|}\right) - i\pi\right)$$

and to obtain the contribution from Fig. 2.1(b) we simply replace $s$ by $u$. Now since $u/t$ is positive this diagram does *not* possess an imaginary part in leading order. It simply has the contribution proportional to

$$\frac{1}{u}\ln\left(\frac{u}{t}\right).$$

Since $u \approx -s$ the logarithms cancel and we are left with the purely imaginary part from Fig. 2.1(a).

## 2.3 Next-to-leading order contribution

In this section we are interested in those contributions which are of order $g^2 \ln s$ relative to the leading order contribution (calculated in the last section). This means that the vast majority of the higher order graphs can be neglected. The only diagram contributing to the leading logarithm in this order is shown in Fig. 2.3: the so-called one-rung ladder diagram (this will unfortunately *not* be true in the case of QCD). We shall explain why other types of diagram are suppressed at the end of this section. We start as before by considering the colour factor. This gives us a factor of $N$ for each $SU(N)$, relative to the leading order contribution, as can be seen from the relation

$$\mathrm{Tr}(T^c T^d) f_{ace} f_{bde} = N \mathrm{Tr}(T^a T^b). \quad (2.9)$$

https://doi.org/10.1017/9781009290111.004 Published online by Cambridge University Press

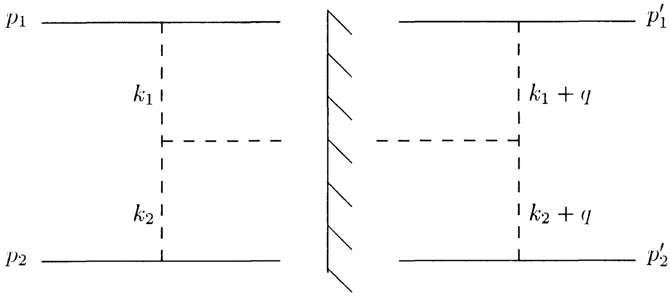


Fig. 2.3. One-rung ladder diagram.

We calculate the imaginary part of this diagram using the same dispersive technique used in the preceding section, i.e.

$$\Im\mathrm{m}\mathcal{A}_{(2.3)} = \frac{1}{2}\int d\left(P.S.^3\right) \mathcal{A}_1^{(g)}(k)\mathcal{A}_1^{(g)\dagger}(k-q) \qquad (2.10)$$

where

$$\mathcal{A}_1^{(g)}(k) = g^3m^3\frac{1}{(k_1^2-m^2)(k_2^2-m^2)}. \qquad (2.11)$$

Once again we write the momenta of the exchanged gluons ($k_1$ and $k_2$) in terms of Sudakov variables $\rho_1, \lambda_1, \mathbf{k_1}, \rho_2, \lambda_2, \mathbf{k_2}$, and the three-body phase-space integral becomes

$$\begin{aligned}\int d\left(P.S.^3\right) &= \frac{s^2}{128\pi^5}\int d\rho_1 d\lambda_1 d^2\mathbf{k_1} d\rho_2 d\lambda_2 d^2\mathbf{k_2} \\ &\quad \delta(-s(1-\rho_1)\lambda_1-\mathbf{k_1^2})\,\delta(s(1+\lambda_2)\rho_2-\mathbf{k_2^2}) \\ &\quad \delta(s(\rho_1-\rho_2)(\lambda_1-\lambda_2)-(\mathbf{k_1}-\mathbf{k_2})^2). \qquad (2.12)\end{aligned}$$

Since $p_1^2=0$ and $p_2^2=0$, we expect a symmetry in $\mathbf{k_1}$ and $\mathbf{k_2}$, so, as before, we expect all the transverse momenta to have magnitudes which are of the order of the larger of $m$ and $\sqrt{|t|}$. The three-body phase-space integral gives a leading logarithm term $\propto \ln s$ with $s$ scaled by the squared transverse momenta. To leading logarithm order it does not matter exactly what values these transverse momenta that scale the logarithms are. Thus when considering the kinematic limits for the variables $\rho_{1,2}$ and $\lambda_{1,2}$ we can set

$$\mathbf{k_1^2} = \mathbf{k_2^2} = (\mathbf{k_1}-\mathbf{k_2})^2 = \mathbf{k}^2,$$

https://doi.org/10.1017/9781009290111.004 Published online by Cambridge University Press

where $\mathbf{k}$ is a generic transverse momentum whose magnitude is much smaller than $\sqrt{s}$. This situation is in marked contrast to that of deep inelastic scattering (away from very low Bjorken-$x$), where at one end of the ladder† there is a very off-shell photon with squared momentum $-Q^2$ and the leading $\ln Q^2$ contribution is dominated by the region of phase space in which the transverse momenta are strongly ordered up the ladder.

The energies of the cut lines in Fig. 2.3 must be positive *in any Lorentz frame*. This means that the components in the direction of $p_1$ and $p_2$ must both be positive for all external lines. This leads to kinematic limits

$$\begin{array}{ccccccc} 1 > & \rho_1 & > & \rho_2 & > & 0 \\ 1 > & |\lambda_2| & > & |\lambda_1| & > & 0 \end{array} \tag{2.13}$$

(note that $\lambda_{1,2}$ are negative). We shall argue below that for the leading logarithm these inequalities may be replaced by strong orderings, i.e.

$$\begin{array}{ccccc} 1 \gg & \rho_1 & \gg & \rho_2 \\ 1 \gg & |\lambda_2| & \gg & |\lambda_1|. \end{array} \tag{2.14}$$

In this approximation, the three-body phase-space integral may be replaced by

$$\begin{aligned} \int d\left(P.S.^3\right) &= \frac{s^2}{128\pi^5}\int d\rho_1 d\lambda_1 d^2\mathbf{k_1} d\rho_2 d\lambda_2 d^2\mathbf{k_2} \\ &\quad \times \delta(-s\lambda_1 - \mathbf{k}^2)\ \delta(s\rho_2 - \mathbf{k}^2) \\ &\quad \times \delta(-s(\rho_1\lambda_2) - \mathbf{k}^2). \end{aligned} \tag{2.15}$$

Now performing the integrations over $\lambda_{1,2}$ by absorbing two of the delta functions we end up with

$$\int d\left(P.S.^3\right) = \frac{1}{128\pi^5}\int_{\rho_2}^{1} \frac{d\rho_1}{\rho_1} d\rho_2 d^2\mathbf{k_1} d^2\mathbf{k_2} \delta(s\rho_2 - \mathbf{k}^2). \tag{2.16}$$

We can easily perform the integration over $\rho_2$ by absorbing the remaining delta function and then the $\ln s$ term arises from the integral over $\rho_1$, i.e.

$$\int_{\mathbf{k}^2/s}^{1} \frac{d\rho_1}{\rho_1}.$$

† Scaling violations in deep inelastic scattering are driven by ladder diagrams in QCD as embodied in the DGLAP equations (see Chapter 6).

https://doi.org/10.1017/9781009290111.004 Published online by Cambridge University Press

It is this integral which, in the leading logarithm approximation, is dominated by the region $1 \gg \rho_1 \gg \mathbf{k}^2/s$. We can see this by introducing two parameters, $\epsilon_1$ and $\epsilon_2$, such that $1 \gg \epsilon_1,\, \epsilon_2 \gg \mathbf{k}^2/s$ and splitting the integral up into three parts:

$$\begin{aligned}\int_{\mathbf{k}^2/s}^{1} \frac{d\rho_1}{\rho_1} &= \left[\int_{\mathbf{k}^2/s}^{\mathbf{k}^2/s\epsilon_1} + \int_{\mathbf{k}^2/s\epsilon_1}^{1/\epsilon_2} + \int_{1/\epsilon_2}^{1}\right] \frac{d\rho_1}{\rho_1} \\ &= -\ln \epsilon_1 + \left(\ln\left(\epsilon_1/\epsilon_2\right) + \ln\left(s/\mathbf{k}^2\right)\right) + \ln \epsilon_2 .\end{aligned}$$

Since $s/\mathbf{k}^2 \gg 1/\epsilon_1, 1/\epsilon_2$ this is dominated by the middle part of the integral for which $1 \gg \rho_1 \gg \mathbf{k}^2/s$, as required. This argument may seem a little far fetched, since we are assuming that the $\epsilon_i$ are sufficiently large compared with $\mathbf{k}^2/s$ that we can neglect their logarithms, and it might be felt that this only works when $s$ is extremely large. Nevertheless this is the formal definition of the leading logarithm approximation and corrections are indeed suppressed by powers of $\ln s$. Thus we have justified the assumption of strong ordering in the $\rho$ s which, together with the on-shell conditions for the cut lines, give a similar strong ordering (in the opposite direction) for the $\lambda$ s, thereby justifying the strong inequality Eq.(2.14).

Since we now have $s\rho_1\lambda_2 \approx \mathbf{k}^2$, it follows that

$$\begin{aligned} s\rho_1\lambda_1 &\ll \mathbf{k_1^2} \\ s\rho_2\lambda_2 &\ll \mathbf{k_2^2} \end{aligned}$$

so that $\mathcal{A}_1$ (Eq.(2.11)) may be rewritten

$$\mathcal{A}_1^{(g)}(k) = g^3 m^3 \frac{1}{(\mathbf{k_1^2} + m^2)(\mathbf{k_2^2} + m^2)}. \tag{2.17}$$

Now we introduce $f_1$ in analogy with $f_0$ (Eq.(2.7)), i.e.

$$\Im m \mathcal{A}_{(2.3)} = \frac{(N^2-1)}{16N^4} \frac{g^4 m^4}{16\pi^2 s} \int d^2\mathbf{k_1} f_1(s, \mathbf{k_1}, \mathbf{q}), \tag{2.18}$$

where

$$\begin{aligned} f_1(s, \mathbf{k_1}, \mathbf{q}) &= \frac{g^2 m^2 N^2 s}{2(2\pi)^3} \int_0^1 d\rho_2 \int_{\rho_2}^{1} \frac{d\rho_1}{\rho_1}\, \delta(s\rho_2 - \mathbf{k}^2) \int d^2\mathbf{k_2} \\ &\times \frac{1}{(\mathbf{k_1^2} + m^2)(\mathbf{k_2^2} + m^2)} \frac{1}{\left((\mathbf{k_1} - \mathbf{q})^2 + m^2\right)\left((\mathbf{k_2} - \mathbf{q})^2 + m^2\right)}. \end{aligned} \tag{2.19}$$

With a view to application in the more complicated case of QCD, rather than performing the $\rho$-integral, we introduce the technique

https://doi.org/10.1017/9781009290111.004 Published online by Cambridge University Press

of Mellin transforms (a survival kit on Mellin transforms appears in the appendix to this chapter). This has the effect of unravelling the nested integrals in the $\rho$ s. Thus we define the Mellin transform of $f_1(s, \mathbf{k_1}, \mathbf{q})$ to be $\mathcal{F}_1(\omega, \mathbf{k_1}, \mathbf{q})$ given by

$$\mathcal{F}_1(\omega, \mathbf{k_1}, \mathbf{q}) = \int_1^\infty d\left(\frac{s}{\mathbf{k}^2}\right)\left(\frac{s}{\mathbf{k}^2}\right)^{-\omega-1} f_1(s, \mathbf{k_1}, \mathbf{q}).$$

In this definition we have normalized $s$ by the square of the typical transverse momentum, $\mathbf{k}$, in order to be able to keep track of dimensions. Recall that for the leading logarithm approximation the exact normalization does not matter as long as it is a scale which is small compared with $s$.

We perform the integration over $s$, and obtain

$$\begin{aligned}\mathcal{F}_1(\omega, \mathbf{k_1}, \mathbf{q}) &= \frac{g^2 m^2 N^2}{2(2\pi)^3}\int_0^1 d\rho_2 \int_{\rho_2}^1 \frac{d\rho_1}{\rho_1}\,\rho_2^{\omega-1}\int d^2\mathbf{k_2} \\ &\times \frac{1}{(\mathbf{k_1^2}+m^2)(\mathbf{k_2^2}+m^2)}\frac{1}{((\mathbf{k_1}-\mathbf{q})^2+m^2)((\mathbf{k_2}-\mathbf{q})^2+m^2)}. \end{aligned} \tag{2.20}$$

The integrations over the $\rho$ s are unravelled by the change of variables

$$\begin{aligned}\tau_1 &= \rho_1 \\ \tau_1\tau_2 &= \rho_2.\end{aligned}$$

The limits of integration are now simply

$$0 < \tau_{1,2} < 1$$

and the Jacobian for this change of integration variables is $\rho_1$, so we obtain

$$\begin{aligned}\mathcal{F}_1(\omega, \mathbf{k_1}, \mathbf{q}) &= \frac{g^2 m^2 N^2}{2(2\pi)^3}\int_0^1 d\tau_1\,\tau_1^{\omega-1}\int_0^1 d\tau_2\,\tau_2^{\omega-1}\int d^2\mathbf{k_2} \\ &\times \frac{1}{(\mathbf{k_1^2}+m^2)(\mathbf{k_2^2}+m^2)}\frac{1}{((\mathbf{k_1}-\mathbf{q})^2+m^2)((\mathbf{k_2}-\mathbf{q})^2+m^2)},\end{aligned}$$

i.e.

$$\begin{aligned}\omega^2\mathcal{F}_1(\omega, \mathbf{k_1}, \mathbf{q}) &= \frac{g^2 m^2 N^2}{2(2\pi)^3}\int d^2\mathbf{k_2} \\ &\times \frac{1}{(\mathbf{k_1^2}+m^2)(\mathbf{k_2^2}+m^2)}\frac{1}{((\mathbf{k_1}-\mathbf{q})^2+m^2)((\mathbf{k_2}-\mathbf{q})^2+m^2)}.\end{aligned} \tag{2.21}$$

https://doi.org/10.1017/9781009290111.004 Published online by Cambridge University Press

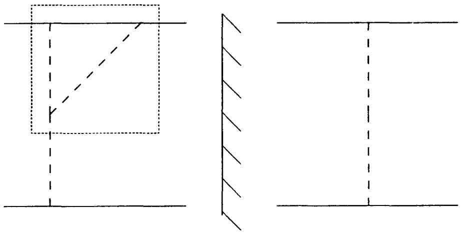

Fig. 2.4. A vertex correction diagram.

We shall write this in a suggestive form as

$$\omega\mathcal{F}_1(\omega,\mathbf{k_1},\mathbf{q}) = \frac{g^2m^2N^2}{2(2\pi)^3}\int d^2\mathbf{k_2} \times \frac{1}{(\mathbf{k}_2^2+m^2)}\frac{1}{((\mathbf{k_2}-\mathbf{q})^2+m^2)}\mathcal{F}_0(\omega,\mathbf{k_1},\mathbf{q}), \quad (2.22)$$

where $\mathcal{F}_0(\omega,\mathbf{k_1},\mathbf{q}) = \omega^{-1}f_0(\mathbf{k_1},\mathbf{q})$ is the Mellin transform of $f_0(\mathbf{k_1},\mathbf{q})$, given in Eq.(2.8).

An example of a diagram that has been neglected is shown in Fig. 2.4, which is a vertex correction to the leading order contribution. This certainly contains an extra $g^2$ relative to the leading order graph, but no extra $\ln s$, since the vertex correction (shown in the dotted box in Fig. 2.4) cannot depend upon $s$ as the squared momentum of the lines coming into the vertex is either zero or $k^2$, which is of order $t$ (i.e. the on-shell condition of the cut upper quark line means we cannot strongly order the Sudakov components of the $t$-channel gluons). This is the case for all diagrams which have vertex or self-energy insertions.

There are also other diagrams which one can draw to this order which do not contribute in the leading logarithm approximation. The first is shown in Fig. 2.5, which is a vertex correction diagram, but with three cut lines. The momenta $k_1$ and $k_2$ are still ordered as discussed above, so

$$|\lambda_2| \gg \frac{\mathbf{k}^2}{s}$$

and the squared momentum of the upper quark line on the right hand side of the cut, $(p_1-k_2)^2$, is of order $|\lambda_2|s \gg \mathbf{k}^2$. This highly virtual quark will give a large denominator (compared with the

https://doi.org/10.1017/9781009290111.004 Published online by Cambridge University Press

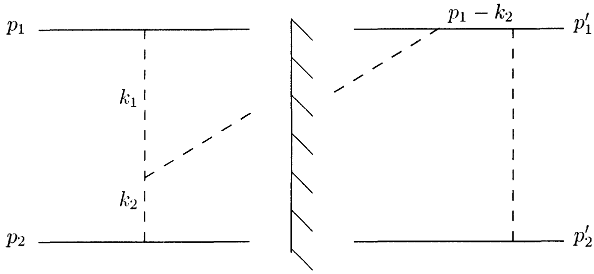


Fig. 2.5. A (cut) vertex correction diagram.

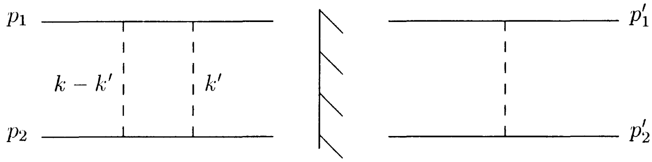


Fig. 2.6. A three gluon exchange diagram.

denominators from Fig. 2.3, which are all of order $\mathbf{k}^2$) and the graph is therefore suppressed and does not contribute in leading logarithm approximation. This is a feature of the scalar theory and does not hold in the case of QCD, where momenta arising from the vertices can compensate for this hard propagator. Furthermore, we neglect diagrams in which there are fermion loops (e.g. a diagram in which there are three quarks and an antiquark rather than two quarks and two gluons in the intermediate state). In the present case we argue that the colour factor is suppressed by $1/N^2$. However, in the case of QCD we shall argue in the next chapter that all such fermion loop diagrams are sub-leading in $\ln s$.

The other type of diagram that we have to consider is the three gluon exchange diagram, which is shown in Fig. 2.6. In the diagram the cut is to the right of two of the gluons (there is also a contribution in which the two gluons on the left of the cut are crossed, and a further contribution to the imaginary part of the diagram where the cut is to the left of two gluons). However, for this type of diagram there is very little phase space when all the

https://doi.org/10.1017/9781009290111.004 Published online by Cambridge University Press

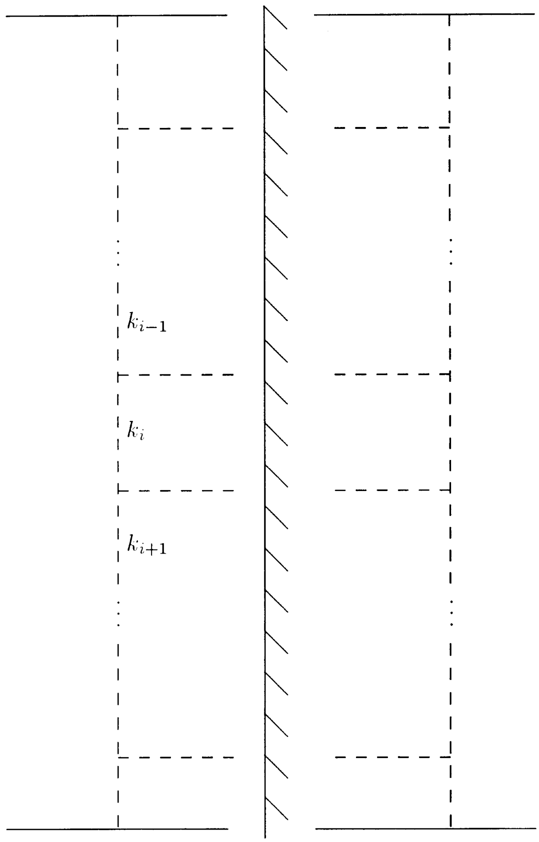


Fig. 2.7. $n$-rung ladder diagram.

denominators are small and so the amplitudes are suppressed by a power of $m^2/s$, compared with diagrams with only two gluons exchanged. These diagrams may therefore be neglected. This is also a feature which holds in the scalar theory but not in QCD.

## 2.4 The $n$-rung ladder diagram

It is now relatively straightforward to generalize the above discussion to any order in perturbation theory. The order $(g^2 \ln s)^n$ correction to the leading order approximation is given by the $n$-rung

https://doi.org/10.1017/9781009290111.004 Published online by Cambridge University Press

uncrossed ladder diagram (Fig. 2.7) whose amplitude has an imaginary part:

$$\Im\mathrm{m}\mathcal{A}_{(2.7)} = \frac{1}{2}\int d\left(P.S.^{(n+2)}\right)\mathcal{A}_n^{(g)}(k)\mathcal{A}_n^{(g)\dagger}(k-q) \qquad (2.23)$$

where

$$\mathcal{A}_n^{(g)}(k) = (-gm)^{n+2}\prod_{i=1}^{n+1}\frac{1}{(k_i^2-m^2)} \qquad (2.24)$$

up to a colour factor. The group theory (see Eq.(2.9)) gives a factor of $N^2$ for each rung relative to the leading order colour factor (Eq.(2.3)).

The momentum of the $i$th upright section of the ladder is written

$$k_i^\mu = \rho_i p_1^\mu + \lambda_i p_2^\mu + k_{i\perp}^\mu$$

with

$$k_{i\perp}^\mu = (0,0,\mathbf{k_i})$$

and the $(n+2)$-body phase-space integral is then

$$\int d\left(P.S.^{(n+2)}\right) = \frac{s^{n+1}}{2^{4n+3}\pi^{3n+2}}\int\prod_{i=1}^{n+1}d\rho_i d\lambda_i d^2\mathbf{k_i}$$
$$\times\prod_{j=1}^{n}\delta(s(\rho_j-\rho_{j+1})(\lambda_j-\lambda_{j+1})-(\mathbf{k_j}-\mathbf{k_{j+1}})^2)$$
$$\times\,\delta(-s(1-\rho_1)\lambda_1-\mathbf{k_1^2})\delta(s(1+\lambda_{n+1})\rho_{n+1}-\mathbf{k_{n+1}^2}). \qquad (2.25)$$

Again the symmetry between $p_1$ and $p_2$ (the top and the bottom of the ladder) tells us that the phase-space integral is dominated by the region in which the transverse momenta of the vertical lines (and the horizontal cut lines) are all of order $\mathbf{k}^2$, which is of the order of the larger of $m^2$ and $|t|$. Furthermore the integral over the Sudakov variables $\rho_i$ and $\lambda_i$ comes from the region

$$\rho_i \gg \rho_{i+1}$$
$$|\lambda_{i+1}| \gg |\lambda_i|$$

and in this region we have $k_i^2 \approx -\mathbf{k_i^2}$, so that $\mathcal{A}_n^{(g)}(k)$ may be written

$$\mathcal{A}_n^{(g)}(k) = -(gm)^{n+2}\prod_{i=1}^{n+1}\frac{1}{(\mathbf{k_i^2}+m^2)}. \qquad (2.26)$$

https://doi.org/10.1017/9781009290111.004 Published online by Cambridge University Press

The phase-space integral (after integrating the $\lambda_i$ by absorbing the delta functions which put the cut lines on mass-shell) is

$$\int d\left(P.S.^{(n+2)}\right) = \frac{1}{2^{4n+3}\pi^{3n+2}} \prod_{i=1}^{n} \int_{\rho_{i+1}}^{1} \frac{d\rho_i}{\rho_i} \prod_{j=1}^{n+1} d^2\mathbf{k_j} \times d\rho_{n+1}\, \delta(s\rho_{n+1} - \mathbf{k}^2). \tag{2.27}$$

The nested integrals over the $\rho_i$ give the leading logarithm contribution proportional to $(\ln s)^n/n!$. We define $f_n$, in analogy with $f_0$ and $f_1$, by

$$\Im m\mathcal{A}_{(2.7)} = \frac{(N^2-1)^2}{16N^4} \frac{g^4 m^4}{16\pi^2 s} \int d^2\mathbf{k_1} f_n(s, \mathbf{k_1}, \mathbf{q}) \tag{2.28}$$

where

$$f_n(s, \mathbf{k_1}, \mathbf{q}) = \left(\frac{g^2 m^2 N^2}{2(2\pi)^3}\right)^n \prod_{i=1}^{n} \int_{\rho_{i+1}}^{1} \frac{d\rho_i}{\rho_i} \int_0^1 d\rho_{n+1} \prod_{j=2}^{n+1} d^2\mathbf{k_j} \times \prod_{m=1}^{n+1} \frac{1}{(\mathbf{k_m^2}+m^2)((\mathbf{k_m}-\mathbf{q})^2+m^2)}\, s\, \delta(s\rho_{n+1} - \mathbf{k}^2). \tag{2.29}$$

We now take the Mellin transform, integrate over $s$ (absorbing the remaining delta function) and change variables from $\rho_i$ to $\tau_i$, where

$$\tau_i = \frac{\rho_i}{\rho_{i-1}}$$

(with $\rho_0 = 1$). The limits on the $\tau$ integrals are $0 < \tau_i < 1$ and the Jacobian for this change of integration variables is $\rho_1 \rho_2 \cdots \rho_n$. Hence

$$\begin{aligned} \mathcal{F}_n(\omega, \mathbf{k_1}, \mathbf{q}) &= \left(\frac{g^2 m^2 N^2}{2(2\pi)^3}\right)^n \prod_{i=1}^{n+1} \int_0^1 \tau_i^{\omega-1}\, d\tau_i \prod_{j=2}^{n+1} d^2\mathbf{k_j} \\ &\quad \times \prod_{m=1}^{n+1} \frac{1}{(\mathbf{k_m^2}+m^2)((\mathbf{k_m}-\mathbf{q})^2+m^2)} \\ &= \left(\frac{g^2 m^2 N^2}{2(2\pi)^3}\right)^n \frac{1}{\omega^{n+1}} \left(\int d^2\mathbf{k} \frac{1}{(\mathbf{k}^2+m^2)((\mathbf{k}-\mathbf{q})^2+m^2)}\right)^n \\ &\quad \times \frac{1}{(\mathbf{k_1^2}+m^2)((\mathbf{k_1}-\mathbf{q})^2+m^2)}. \end{aligned} \tag{2.30}$$

Note that the factor $(1/\omega)^{n+1}$ is the Mellin transform of $(\ln s)^n/n!$.

https://doi.org/10.1017/9781009290111.004 Published online by Cambridge University Press

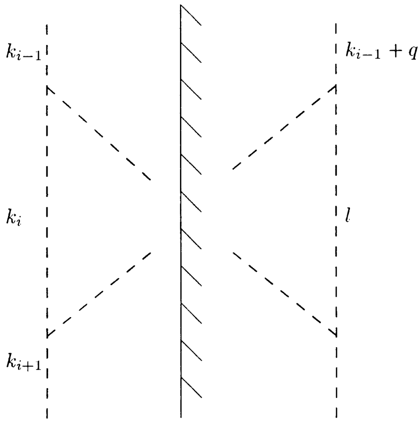


Fig. 2.8. A section of a crossed ladder diagram.

Crossed ladder diagrams do not contribute in leading logarithm approximation. A section of such a ladder is shown in Fig. 2.8. In this diagram the momentum on the right of the cut, marked $l$, is given by

$$l = k_{i-1} + k_{i+1} - k_i - q.$$

In the limit $\rho_{i-1} \gg \rho_i \gg \rho_{i+1}$ and $|\lambda_{i+1}| \gg |\lambda_i| \gg |\lambda_{i-1}|$, this propagator gives rise to a denominator which is of order

$$l^2 \approx s\lambda_{i+1}\rho_{i-1}$$

but $s\lambda_{i+1}$ is of order $\mathbf{k}^2/\rho_i$ (from the mass-shell condition of the $i$th cut line) and so we have

$$l^2 \approx \frac{\rho_{i-1}}{\rho_i}\mathbf{k}^2,$$

which is much larger than $\mathbf{k}^2$ (since $\rho_{i-1} \gg \rho_i$). Thus there is a large denominator, which suppresses the contribution from this diagram so that it no longer contributes in leading logarithm approximation. Once again QCD does not possess this rather convenient feature.

The series, $\sum_{n=0}^{\infty} \mathcal{F}_n(\omega, \mathbf{k_1}, \mathbf{q})$, is a simple geometrical series (see Eq.(2.30)) and can be summed to give

$$\mathcal{F}(\omega, \mathbf{k}, \mathbf{q}) = \frac{1}{(\mathbf{k}^2 + m^2)((\mathbf{k}-\mathbf{q})^2 + m^2)(\omega - 1 - \alpha_P(t))}, \quad (2.31)$$

https://doi.org/10.1017/9781009290111.004 Published online by Cambridge University Press

where

$$\alpha_P(t) = -1 + \frac{g^2 m^2 N^2}{2(2\pi)^3} \int d^2\mathbf{k}' \frac{1}{(\mathbf{k}'^2 + m^2)((\mathbf{k}' - \mathbf{q})^2 + m^2)} \quad (2.32)$$

(with $t = -\mathbf{q}^2$). The integral over the transverse momentum is readily computed. For small $t$ ($|t| \ll m^2$) we have

$$\alpha_P(t) \approx -1 + \frac{g^2 N^2}{16\pi^2}\left(1 + \frac{t}{6m^2}\right). \quad (2.33)$$

The trajectory rapidly becomes non-linear as $|t|$ becomes of order $m^2$. Thus we see that $\mathcal{F}(\omega, \mathbf{k}, \mathbf{q})$ has a simple pole in $\omega$ at $\omega = 1 + \alpha_P(t)$.

## 2.5 The integral equation

Although we already have a solution for $\mathcal{F}(\omega, \mathbf{k}, \mathbf{q})$, in preparation for the case of QCD it is useful to establish an integral equation which gives the same result. Such an integral equation is shown schematically in Fig. 2.9. It is an implicit equation with $\mathcal{F}(\omega, \mathbf{k}, \mathbf{q})$ appearing on both sides. Basically it tells us that $\mathcal{F}$ is equal to the leading order term plus $\mathcal{F}$ with an extra rung added. The extra rung introduces a coupling constant factor of $g^2m^2$, a colour factor of $N^2$, two propagators for the extra internal lines, $1/(\mathbf{k}'^2 + m^2)$ and $1/((\mathbf{k}' - \mathbf{q})^2 + m^2)$, and an extra phase-space integral, which in the Mellin transform representation gives a factor of $1/(2(2\pi)^3\omega)$ combined with an integral over the transverse momentum $d^2\mathbf{k}'$. Thus the integral equation is

$$\begin{aligned} \omega\mathcal{F}(\omega, \mathbf{k}, \mathbf{q}) &= \frac{1}{(\mathbf{k}^2 + m^2)((\mathbf{k} - \mathbf{q})^2 + m^2)} \\ &+ \frac{g^2 m^2 N^2}{2(2\pi)^3\omega} \int d^2\mathbf{k}' \frac{\mathcal{F}(\omega, \mathbf{k}, \mathbf{q})}{(\mathbf{k}'^2 + m^2)((\mathbf{k}' - \mathbf{q})^2 + m^2)}. \end{aligned} \quad (2.34)$$

We see that if we insert the first term on the right hand side into $\mathcal{F}$ in the second term, we obtain the one-rung ladder contribution, and inserting this into $\mathcal{F}$ in the second term gives the two-rung contribution, etc. By iteration we thus see that the integral equation generates all the ladder diagrams.

The integral equation of course gives the same solution as Eq.(2.31).

https://doi.org/10.1017/9781009290111.004 Published online by Cambridge University Press

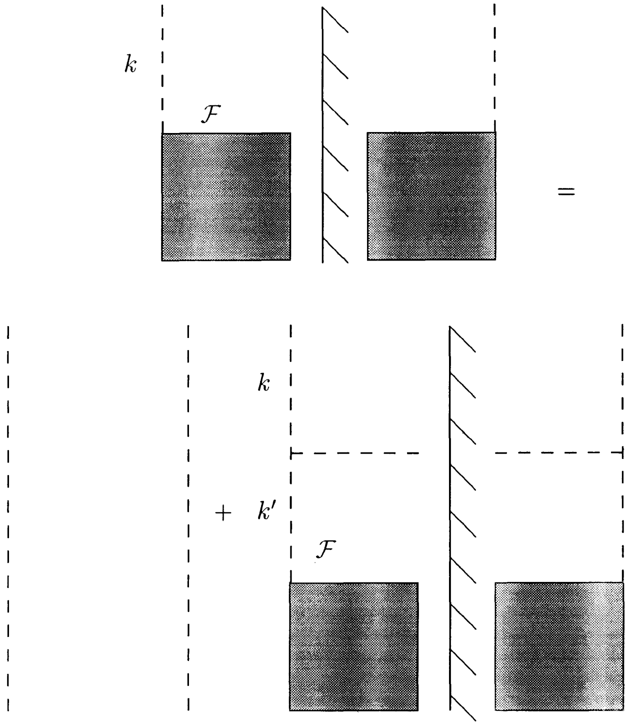


Fig. 2.9. The integral equation.

## 2.6 The Pomeron

After this rather tortuous route we now come to the solution for the amplitude $\mathcal{A}(s,t)$ for the colour singlet exchange. Inverting the Mellin transform we have

$$\begin{aligned} \Im m\mathcal{A}(s,t) &= \frac{(N^2-1)^2}{16N^4}\frac{g^4m^4}{16\pi^2 s} \\ &\times \int d^2\mathbf{k}\frac{1}{(\mathbf{k}^2+m^2)((\mathbf{k}-\mathbf{q})^2+m^2)}\left(\frac{s}{|t|}\right)^{1+\alpha_P(t)}, \end{aligned} \tag{2.35}$$

with $\alpha_P(t)$ given by Eq.(2.32) and we have substituted $|t|$ for $\mathbf{k}^2$ in the normalization of $s$, which we may do without affecting the leading logarithms.

https://doi.org/10.1017/9781009290111.004 Published online by Cambridge University Press

Let us write this as

$$\Im m\mathcal{A}(s,t) = \frac{\mathcal{C}}{s}\left(\frac{s}{|t|}\right)^{\epsilon_P(t)},$$

where

$$\epsilon_P(t) = 1 + \alpha_P(t)$$

(note that $\epsilon_P(t)$ is of order $g^2$). Up to corrections which are of order $g^2$, this is the imaginary part of

$$\begin{aligned}\mathcal{A}(s,t) &= \left(\frac{s}{-t}\right)^{\epsilon_P(t)} \frac{\mathcal{C}}{s\pi\epsilon_P(t)}\left[\cos\pi\epsilon_P(t) + i\sin\pi\epsilon_P(t)\right] \\ &\approx \frac{\mathcal{C}}{\pi\epsilon_P(t)s}\left(\frac{s}{t}\right)^{\epsilon_P(t)}.\end{aligned}$$

Remember that we must add the contribution from the crossed amplitude in which $s$ is replaced by $u$. Thus the entire contribution is

$$\begin{aligned}\mathcal{A}(s,t) &= \frac{\mathcal{C}}{\pi\epsilon_P(t)s}\left(\frac{s}{t}\right)^{\epsilon_P(t)} \\ &+ \frac{\mathcal{C}}{\pi\epsilon_P(t)u}\left(\frac{u}{t}\right)^{\epsilon_P(t)}.\end{aligned}$$

In the Regge limit $u \approx -s$ and so we see that the real parts cancel in leading logarithm order and we are left with an amplitude that is *purely imaginary* and given by Eq.(2.35).

We have thus succeeded in deriving the Pomeron in this particular field theory.

## 2.7 Summary

Let us summarize the important features of Pomeron exchange in the scalar model discussed in this chapter.

- In the scalar model with cubic interactions described in Section 2.1, the leading logarithm contributions to the imaginary part of the amplitude come from uncrossed ladder diagrams, with a cut through the rungs. The cut lines are integrated over the relevant phase space.
- We use Sudakov variables to describe the momentum $k_i$ of the $i$th vertical line on the left of the ladder by

$$k_i^\mu = \rho_i p_1^\mu + \lambda_i p_2^\mu + k_{i\perp}^\mu$$

https://doi.org/10.1017/9781009290111.004 Published online by Cambridge University Press

with

$$k^{\mu}_{i\perp} = (0, 0, \mathbf{k_i}).$$

For the right hand side of the ladder the transverse momentum $\mathbf{k_i}$ is replaced by $(\mathbf{k_i} - \mathbf{q})$ (in the Regge limit, $|t| \ll s$).

- The phase-space integral is dominated by the region in which the transverse momenta all have the same order of magnitude, which is denoted by $\mathbf{k}$, such that $\mathbf{k}^2$ is of the order of the larger of $m^2$ and $|t|$.
- The leading logarithm part of the integral over the longitudinal components comes from the region

$$\begin{aligned} \rho_i &\gg \rho_{i+1} \\ |\lambda_{i+1}| &\gg |\lambda_i| \end{aligned}$$

and in this region the momenta of the vertical lines are dominated by their transverse components so that $k_i^2 \approx -\mathbf{k_i^2}$.

- After integrating over the $\lambda_i$ and absorbing the delta functions which give the on-shell condition for the cut lines, the remaining integration over the $\rho_i$ are nested integrals which are easily unravelled by taking the Mellin transform.
- An integral equation can be established for the Mellin transform of the imaginary part of the amplitude. The sum of all ladder diagrams is generated if the integral equation is solved iteratively.
- The integral equation has a solution for which the Mellin transform has a simple pole at $\omega = 1 + \alpha_P(t)$, where $\alpha_P(t)$ is given by Eq.(2.32).
- The real part of the amplitude is readily reconstructed from the imaginary part. However when the contribution from the crossed process obtained by interchanging $s$ and $u$ is added, the leading order contribution of the real part cancels, leaving a purely imaginary amplitude.

## 2.8 Appendix

### Mellin transforms

**Definition:**

The Mellin transform, $\mathcal{F}(\omega)$ of the function $f(s)$ is given by

$$\mathcal{F}(\omega) = \int_1^\infty d\left(\frac{s}{\mathbf{k}^2}\right)\left(\frac{s}{\mathbf{k}^2}\right)^{-\omega-1} f(s) \qquad \text{(A.2.1)}$$

https://doi.org/10.1017/9781009290111.004 Published online by Cambridge University Press

and its inverse is given by

$$f(s) = \frac{1}{2\pi i}\int_C d\omega \left(\frac{s}{\mathbf{k}^2}\right)^{\omega} \mathcal{F}(\omega), \qquad (A.2.2)$$

where the contour $C$ is to the right of all $\omega$-plane singularities of $\mathcal{F}(\omega)$.

**Useful examples:**
If $f(s)$ is of the form

$$f(s) = s^{\alpha} g(s),$$

then the Mellin transform $\mathcal{F}(\omega)$ is given by

$$\mathcal{F}(\omega) = \left(\mathbf{k}^2\right)^{\alpha} \mathcal{G}(\omega - \alpha), \qquad (A.2.3)$$

where $\mathcal{G}(\omega)$ is the Mellin transform of $g(s)$.

If $g(s) = (\ln s)^r$ then its Mellin transform is given by

$$\mathcal{G}(\omega) = \int_1^{\infty} d\left(\frac{s}{\mathbf{k}^2}\right)\left(\frac{s}{\mathbf{k}^2}\right)^{-\omega-1} (\ln s)^r .$$

Changing variables to $y = \omega \ln(s/\mathbf{k}^2)$ we obtain

$$\mathcal{G}(\omega) = \frac{1}{\omega^{r+1}}\int_0^{\infty} y^r e^{-y} dy.$$

The integral on the right hand side is the integral definition of the Euler gamma function, $\Gamma(r+1)$ ($= r!$ for integer $r$). Therefore,

$$\mathcal{G}(\omega) = \frac{\Gamma(r+1)}{\omega^{r+1}}. \qquad (A.2.4)$$

Combining these two results (Eqs.(A.2.3, A.2.4)) we obtain, for the Mellin transform of the function

$$f(s) = (\ln s)^r s^{\alpha},$$

$$\mathcal{F}(\omega) = \left(\mathbf{k}^2\right)^{\alpha} \frac{\Gamma(r+1)}{(\omega-\alpha)^{r+1}}. \qquad (A.2.5)$$

Thus we see that if the function $f(s)$ is a pure power of $s$, then the Mellin transform has a singularity which is a simple pole. If the function $f(s)$ is a power multiplied by (in general non-integer) powers of $\ln s$, then the Mellin transform has a cut singularity. The factor $(\mathbf{k}^2)^{\alpha}$ simply adjusts the dimension. For the high energy behaviour, we are interested in the position and nature of the $\omega$-plane singularities. Note that the Mellin transform of a constant, $\mathcal{C}$, is $\mathcal{C}/\omega$.

https://doi.org/10.1017/9781009290111.004 Published online by Cambridge University Press

It is important to be familiar with these relations in *both* directions, i.e. to be able to perform the inverse Mellin transforms and obtain the $s$-dependence of amplitudes from the singularity structure of the Mellin transforms.

**Convolutions:**
Let $f(s)$ be given in terms of a convolution of a set of $n$ functions, $f_i(s/\mathbf{k}^2)$ $(i = 1 \cdots n)$, by

$$f(s) = \mathbf{k}^2 \prod_{i=1}^{n} \int_{\rho_{i+1}}^{1} \frac{d\rho_i}{\rho_i} f_i \left(\frac{\rho_{i-1}}{\rho_i}\right) \delta(\rho_n s - \mathbf{k}^2) \qquad \text{(A.2.6)}$$

(with $\rho_0 = 1$ and $\rho_{n+1} = 0$). The Mellin transform is given by

$$\begin{aligned} \mathcal{F}(\omega) &= \mathbf{k}^2 \int_1^\infty d\left(\frac{s}{\mathbf{k}^2}\right)\left(\frac{s}{\mathbf{k}^2}\right)^{-\omega-1} \\ &\times \prod_{i=1}^{n} \int_{\rho_{i+1}}^{1} \frac{d\rho_i}{\rho_i} f_i \left(\frac{\rho_{i-1}}{\rho_i}\right) \delta(\rho_n s - \mathbf{k}^2). \end{aligned}$$

Performing the integration over $s/\mathbf{k}^2$ (absorbing the delta function) gives

$$\mathcal{F}(\omega) = \prod_{i=1}^{n} \int_{\rho_{i+1}}^{1} \frac{d\rho_i}{\rho_i} f_i \left(\frac{\rho_{i-1}}{\rho_i}\right) \rho_n^{\omega}.$$

Now change variables from $\rho_i$ to $\tau_i$, where

$$\tau_i = \frac{\rho_i}{\rho_{i-1}},$$

so that $\rho_n = \tau_1 \tau_2 \cdots \tau_n$. The Jacobian for the change of variables is $\rho_1 \rho_2 \cdots \rho_{n-1}$, and we finally obtain

$$\mathcal{F}(\omega) = \prod_{i=1}^{n} \int_0^1 d\tau_i \tau_i^{\omega-1} f_i \left(\frac{1}{\tau_i}\right) = \prod_{i=1}^{n} \mathcal{F}_i(\omega), \qquad \text{(A.2.7)}$$

where $\mathcal{F}_i(\omega)$ are the Mellin transforms of the functions $f_i(s/\mathbf{k}^2)$.

https://doi.org/10.1017/9781009290111.004 Published online by Cambridge University Press